Twin-boundary-mediated flexoelectricity in LaAlO₃

Christopher A. Mizzi ⬤, Binghao Guo ⬤, and Laurence D. Marks[*]

Department of Materials Science and Engineering, Northwestern University, Evanston, Illinois 60208, USA

Flexoelectricity has garnered much attention owing to its ability to bring electromechanical functionality to nonpiezoelectric materials and its nanoscale significance. In order to move towards a more complete understanding of this phenomenon and improve the efficacy of flexoelectric-based devices, it is necessary to quantify microstructural contributions to flexoelectricity. Here we directly measure the flexoelectric response of bulk centrosymmetric LaAlO₃ crystals with different twin-boundary microstructures. We show that twin-boundary flexoelectric contributions are comparable to intrinsic contributions at room temperature and enhance the flexoelectric response by ∼4× at elevated temperatures. Additionally, we observe time-dependent and nonlinear flexoelectric responses associated with strain-gradient-induced twin-boundary polarization. These results are explained by considering the interplay between twin-boundary orientation, beam-bending strain fields, and pinning site interactions, and directly demonstrate that macroscopic flexoelectric responses are very sensitive to structural defects.

I. INTRODUCTION

Inducing an electrical response from a mechanical stimulus (or a mechanical response from an electrical stimulus) in insulators is highly desirable for actuation, sensing, and energy harvesting applications. Historically, such electromechanical functionality has been derived from piezoelectricity (the coupling of strain and polarization), but piezoelectricity faces a fundamental limitation: as a bulk property it only exists in noncentrosymmetric materials [1]. This, coupled with the prevalence of lead in common piezoelectrics, poses a significant materials selection challenge [2].

One approach to overcome these issues is to replace piezoelectric materials with flexoelectric (FxE) materials. Flexoelectricity (the coupling of strain gradient and polarization) allows for the mechanical polarization of all insulators, even those with centrosymmetric space groups, because strain gradients break inversion symmetry [3,4]. Since Ma and Cross discovered large FxE responses in relaxor ferroelectric ceramics [5], research on flexoelectricity in oxides has flourished [3,4]. However, an abundance of fundamental questions persists. Among the most pressing relates to the role of extrinsic contributions to flexoelectricity (e.g., terms related to microstructure, point defects, etc.). Extrinsic contributions are bound to be important in ceramics utilized for electromechanical applications and recent work has shown they can dominate intrinsic (i.e., pure crystallographic) FxE contributions: the overall FxE response has sizeable modifications from free carriers in semiconductors [6], polar nanoregions in relaxor ferroelectrics [7,8], and polar selvedge regions in ferroelectric ceramics [9]. Identifying and separating extrinsic and intrinsic contributions to flexoelectricity is an important step towards improving our fundamental understanding of flexoelectric-

ity, closing the sizable divide between the experimental and theoretical [10–14] states of the field, and substantiating the viability of flexoelectricity for practical applications.

Oxides which when grown at high temperatures are single crystals and develop twin boundaries (TBs) on cooling are well poised to elucidate microstructural FxE contributions because they bridge the gap between single crystals and polycrystalline ceramics. While experiments on such oxides [like SrTiO₃ (STO) [15]] have indicated that TB contributions to flexoelectricity are important, there has been no quantitative analysis of TB FxE contributions, i.e., determining the FxE coefficient of a TB. Moreover, the role of TB microstructure in the overall FxE response of a sample has not been addressed, although recent simulations suggest that ferroelastic microstructure is important in other electromechanical contexts [16–18]. Turning to the specific material of interest herein, LaAlO₃ (LAO) is a rhombohedral "332" perovskite with space group $R\bar{3}c$ at room temperature and atmospheric pressure [19] which twins due to an improper ferroelastic phase transition at 550 °C [20]. It is an ideal material to examine TB effects on flexoelectricity because it is twinned at room temperature and the crystallography of the TBs [21–25], as well as their mechanical response to dynamic mechanical stimuli [20,26–31], have been extensively studied. Understanding flexoelectricity in LAO is also important because it is commonly used as a substrate and film in epitaxial thin-film growth [32,33] (large FxE responses occur at length scales relevant to thin films because of the intrinsic size scaling of strain gradients [34–36]), and there has been recent interest in utilizing FxE couplings to modify the two-dimensional electron gas at the LAO-STO interface [37–40]. More generally, beyond LAO, degrees of freedom often vary rapidly over short distances in the vicinity of domain walls [41]. Consequently, couplings involving gradients can be particularly potent in ferroic materials [42–45], leading to interesting properties that are otherwise forbidden in the bulk of the material [46] such as

---

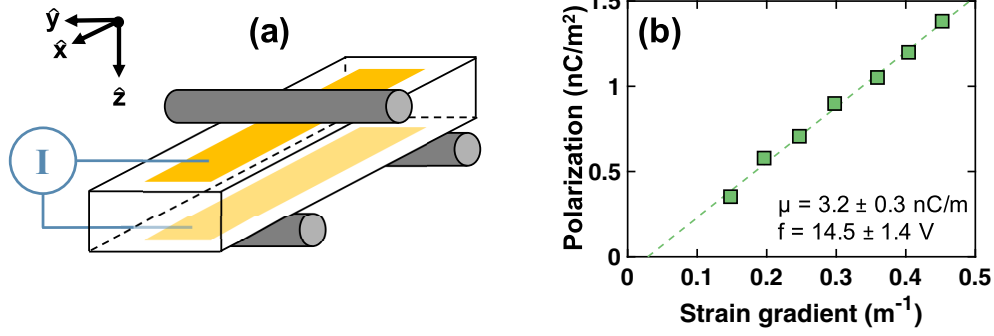*Corresponding author: L-marks@northwestern.edu

FIG. 1. (a) Overview of experimental flexoelectric characterization. The short-circuit current induced by low-frequency three-point bending is measured for a sample cut into a beam geometry. (b) Flexoelectric characterization of a LaAlO$_3$ crystal with no twin boundaries. The strain-gradient-induced polarization in this sample is linear, with an effective flexoelectric coefficient of 3.2 ± 0.3 nC/m (flexocoupling voltage of 14.5 ± 1.4 V). The linear fit is shown as a dashed line. The uncertainty corresponds to the 95% confidence interval of the fit.

TB polarization. While the evidence for static TB polarization [47–53] and electrically driven changes to TB polarization [16–18] in bulk centrosymmetric oxides is compelling, it is unclear how, quantitatively, these static polarizations evolve with strain gradients.

In this paper we show that extrinsic FxE contributions associated with TBs are of the same magnitude as intrinsic contributions to flexoelectricity in LAO. Using a low-frequency beam-bending method we measure the effective FxE coefficient in {100}$_{\text{pseudocubic}}$ LAO crystals with different TB microstructures, demonstrating that strain-gradient-induced TB polarization can yield anelastic and nonlinear FxE responses. Additionally, we report significant microstructure-sensitive enhancements in the effective FxE coefficient of twinned LAO over its single crystal value: $\sim$1.5$\times$ increase at room temperature and $\sim$4$\times$ increase at elevated temperatures. These enhancements are explained by considering the interplay between TB orientation, beam-bending strain fields, and pinning site interactions.

II. METHODS

Throughout this work FxE characterization was performed following Zubko *et al.* [15]: a sample cut into a beam geometry was subjected to low-frequency bending by a dynamic mechanical analyzer while the short-circuit current generated by the FxE effect was measured with a lock-in amplifier [Fig. 1(a)]. In brief (see the Supplemental Material [54] for further details), the short-circuit current (I) is used to calculate the average polarization component along the measurement direction ($\overline{P_z}$) via

$$\overline{P_z} = \frac{I}{2\omega A}, \quad (1)$$

where ω is the oscillatory frequency and A is the electrode area. The displacement at the beam center (u_z) is used to calculate the average strain gradient across the electrode area ($\bar{\epsilon}_{xx,z}$) with

$$\bar{\epsilon}_{xx,z} = 12\, u_z \frac{L-a}{L^3}, \quad (2)$$

where L is the distance between the bending supports, a is the electrode length, and $\epsilon_{ij,k}$ is the gradient of strain ϵ_{ij} with

respect to the k coordinate. The effective FxE coefficient μ_{eff} [15] for a bent cubic beam with {100} faces is given by

$$\overline{P_z} = [\mu_{zzxx}(1-\nu) - \mu_{zzzz}\,\nu]\bar{\epsilon}_{xx,z} = \mu_{\text{eff}}\bar{\epsilon}_{xx,z}, \quad (3)$$

where μ_{ijkl} are the FxE coefficient tensor components [55] and ν is the relevant Poisson ratio. The deviation from a cubic perovskite structure in LAO is small; this approximation is addressed in the Supplemental Material [54].

III. RESULTS AND DISCUSSION

To examine the microstructural contributions to flexoelectricity in LAO, it is necessary to isolate TB effects from crystallographic ones. To this end, we solely focus on {100}$_{\text{pseudocubic}}$ crystals and begin with the FxE characterization of a LAO crystal without twins, which was cut from a twin-free portion of a larger crystal. As shown in Fig. 1(b), TB-free LAO exhibits a linear FxE response with $\mu_{\text{eff}} = 3.2 \pm 0.3$ nC/m. Using the dielectric constant of LAO [20], this corresponds to a flexocoupling voltage of 14.5 ± 1.4 V. This value is in agreement with a recent measurement of the FxE response of LAO using a different approach [40]. Images of the twin-free sample before and after the bending experiments are included in the Supplemental Material [54].

Having established the FxE response of LAO with no twins, TB contributions were studied by measuring flexoelectricity in two samples with different lamellar microstructures. The TB orientations in each sample are described in Fig. 2 and will be referred to as Type I and Type II. As shown in Fig. 2, the initial FxE response of the Type I sample was linear with $\mu_{\text{eff}} = 3.6 \pm 0.2$ nC/m. Additional measurements were then performed while increasing and decreasing the strain gradient (strain gradient cycling). Throughout these measurements the FxE response remained linear and μ_{eff} increased to a steady-state value of 4.8 ± 0.3 nC/m. Measurements performed the next day on the same sample indicated a partial recovery of the initial FxE response, followed by a return to the same steady-state μ_{eff} after strain gradient cycling (Supplemental Material [54]). The Type II sample exhibited qualitatively similar behavior: μ_{eff} increased from 3.1 ± 0.3 nC/m to a steady-state value of 3.5 ± 0.2 nC/m
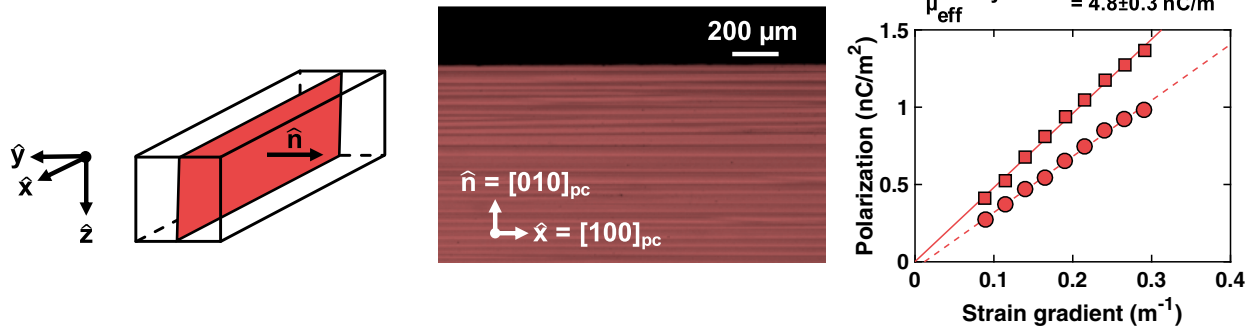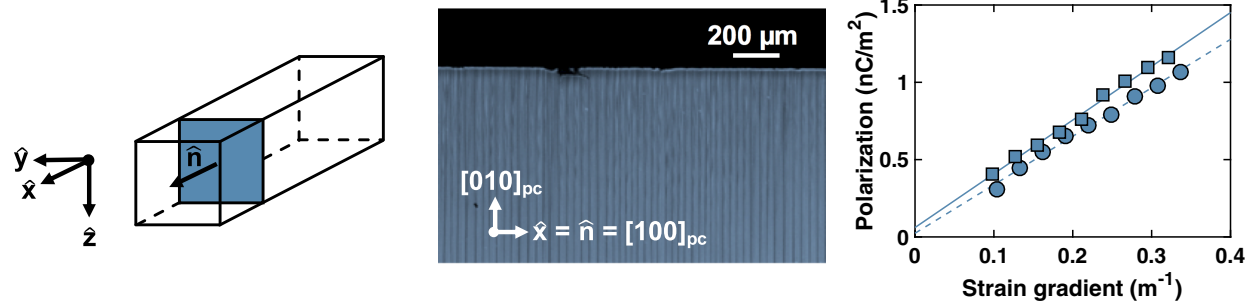
(a) Type I Twin Boundary: $\hat{x} \cdot \hat{n} = 0$

(b) Type II Twin Boundary: $\hat{x} \cdot \hat{n} = 1$

FIG. 2. Flexoelectric characterization of LaAlO₃ crystals with uniform, lamellar twin-boundary microstructures. (a) Type I boundaries have normals ($\hat{n}$) perpendicular to the long axis of the sample ($\hat{x}$) as shown by reflection polarized optical microscopy. The flexoelectric response of the Type I sample was linear and increased to an effective steady-state flexoelectric coefficient of 4.8 ± 0.3 nC/m (flexocoupling voltage of 21.7 ± 1.4 V) after strain gradient cycling. (b) Type II boundaries have normals parallel to the long axis of the sample as shown by reflection polarized optical microscopy. The flexoelectric response of the Type II sample was linear and increased to an effective steady-state flexoelectric coefficient of 3.5 ± 0.2 nC/m (flexocoupling voltage of 15.8 ± 0.9 V) after strain gradient cycling. In both plots, lines are linear fits with circles/dashed lines indicating initial measurements and squares/solid lines indicating steady-state measurements after strain gradient cycling. Uncertainties correspond to the 95% confidence interval of the fit. Images are false-colored for clarity.

after strain gradient cycling, remaining linear throughout the measurements. In both Type I and II samples, postexperiment imaging indicated no permanent changes of the TB microstructure (Supplemental Material [54]).

These results indicate that TBs in LAO are mechanically polarized by strain gradients (Supplemental Material [54] for additional evidence) with FxE contributions that are distinct from, but comparable in magnitude to, the bulk. Further, TB flexoelectricity exhibits anelastic (time-dependent and elastic) and orientation-dependent behavior. The former is a natural consequence of local TB deformation: TBs are pinned and immobile at room temperature so macroscopic TB motion does not occur, but TBs undergo some amount of local elastic or plastic deformation depending on, e.g., the TB microstructure and distribution of pinning sites [26–28,30,31]. The latter is because TB orientation dictates which strain gradient components couple to the measured polarization (e.g., Type I TBs are parallel to the *x-z* plane so FxE contributions to P_z from beam bending can only arise from $\epsilon_{xx,z}$ and $\epsilon_{zz,z}$). By accounting for the different TB orientations in the Type I and II samples, one can estimate the TB FxE coefficients responsible for the FxE enhancements in twinned LAO. As shown in the Supplemental Material [54], μ_{eff} for the Type I and II samples ($\mu_{\mathrm{eff}}^{\mathrm{I,II}}$) are

related to μ_{eff} for the TB-free sample ($\mu_{\mathrm{eff}}^{\mathrm{bulk}}$) via

$$\mu_{\mathrm{eff}}^{\mathrm{I}} = \mu_{\mathrm{eff}}^{\mathrm{bulk}} + \rho_{\mathrm{I}}\, w \left(\mu_{zzxx}^{\mathrm{TB}} - \nu\, \mu_{zzzz}^{\mathrm{TB}} \right), \quad (4)$$

$$\mu_{\mathrm{eff}}^{\mathrm{II}} = \mu_{\mathrm{eff}}^{\mathrm{bulk}} - \rho_{\mathrm{II}}\, w\, \nu \left(\mu_{zzxx}^{\mathrm{TB}} + \mu_{zzzz}^{\mathrm{TB}} \right), \quad (5)$$

where μ_{ijkl}^{TB} are the TB FxE coefficient tensor components, ν is Poisson's ratio [56], ρ_{I} and ρ_{II} are the TB densities in the Type I and II samples (~ 50 mm⁻¹), and w is the TB width (~ 2 nm [57]). From Eqs. (4) and (5) and measurements on the TB-free, Type I, and Type II samples, $\mu_{zzxx}^{\mathrm{TB}} \approx 11 \pm 3.0$ μC/m and $\mu_{zzzz}^{\mathrm{TB}} \approx -18.0 \pm 4.0$ μC/m. These values are comparable to FxE coefficients of bulk polar materials [58] which supports the growing body of literature which indicates LAO TBs are polar [48,49] and could point to TB piezoelectricity [59].

These results provide direct evidence that TBs play a significant role in determining the macroscopic FxE response of twinned materials. To further validate these effects are from TBs, three additional experiments were performed on samples with a mixture of TB orientations (see the Supplemental Material for images [54]). In the first, μ_{eff} was measured as a function of temperature. It is established that increasing temperature enhances TB mobility by providing thermal energy for TBs to escape pinning sites [20,26–31]: at first increasing
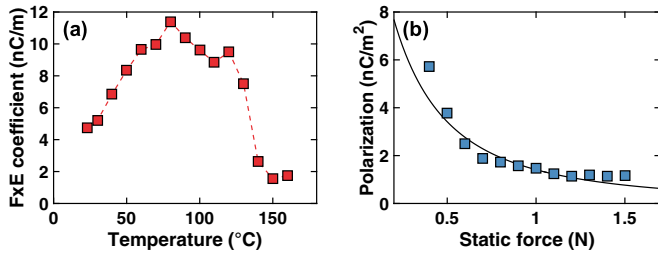
FIG. 3. Flexoelectric measurements in LaAlO$_3$ crystals with a mixture of twin-boundary orientations. (a) The temperature dependence of the flexoelectric coefficient correlates with the known temperature dependence of twin-boundary motion. Dashed lines are visual guides. (b) Flexoelectric polarization at room temperature and fixed dynamic force decreases with increasing static force because of the nonlinear elastic response of twin boundaries. Solid line is a fit using a catenary cable model.

temperature enhances local TB deformations, but after a sample-dependent threshold (typically ~100 °C), large-scale TB motion and annihilation become possible. The temperature dependence shown in Fig. 3(a) correlates well with these trends. Namely, μ_{eff} increases between ~30–100 °C as TBs become more deformable and decreases once TB motion becomes possible, with a maximum corresponding to the onset of motion. We note that unlike the room temperature experiments, increasing temperature led to permanent microstructural changes (Supplemental Material [54]). Also, the FxE response of twinned LAO at elevated temperatures was found to be sensitive to the initial TB microstructure.

The second experiment to confirm our interpretation was measuring the FxE polarization at a constant dynamic force while varying the static force holding the sample in place during three-point bending. Local TB deformation of pinned TBs depends on static force [68], so if TBs contribute to FxE polarization then the FxE polarization should vary with static force (unlike FxE polarization in single crystals which is insensitive to static force) [15]. Figure 3(b) demonstrates that the FxE polarization of twinned LAO at room temperature decreases with increasing static force which is consistent with TB contributions to the FxE response of twinned crystals. As shown in the Supplemental Material [54], this static force dependency is well captured by modeling pinned TBs as catenary cables, where the ends of the cable are pinning sites. Note that this is a standard model for similar problems such as dislocation pinning (e.g., [60]).

The last experiment was measuring the FxE response of a sample with a mixture of Type I and II TBs at fixed static force (comparable to the results in Figs. 1 and 2). As shown in Fig. 4, μ_{eff} increased from an initial value of 3.6 ± 0.1 nC/m to a steady-state value of 4.0 ± 0.2 nC/m (as determined from the first five data points in each data set) after strain gradient cycling. This time dependence is similar to that of the pure Type I and II samples and the steady-state μ_{eff} is between that of the pure Type I and Type II samples, consistent with the mixture of Type I and II TBs present in the sample. Additionally, these measurements indicate a nonlinear FxE response when the strain gradient exceeded ~0.25 m^{-1}. This starkly contrasts with the FxE responses of the other samples
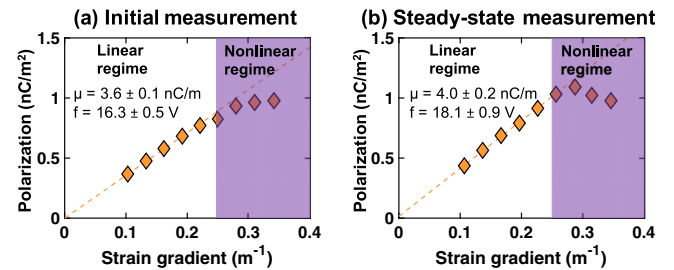

FIG. 4. Flexoelectric characterization of a LaAlO$_3$ crystal with a mixture of Type I and II twin-boundary orientations. (a) The initial flexoelectric response is linear at low strain gradients with an effective flexoelectric coefficient of 3.6 ± 0.1 nC/m (flexocoupling voltage of 16.3 ± 0.5 V), and nonlinear above a strain gradient of ~0.25 m^{-1}. (b) The steady-state flexoelectric response after strain gradient cycling remains linear at low strain gradients with an increased effective flexoelectric coefficient of 4.0 ± 0.2 nC/m (flexocoupling voltage of 18.1 ± 0.9 V). There is pronounced nonlinear behavior above ~0.25 m^{-1}.

which remained linear for all strain gradients used. The non-linearity became more pronounced in the steady state, but a linear FxE response was always recovered by decreasing the strain gradient below ~0.25 m^{-1}. Given the return to a linear FxE response below a certain strain gradient, and that post-experiment imaging confirmed no permanent changes to TB microstructure (Supplemental Material [54]), the nonlinearity is attributed to TB-pinning site interactions. This behavior is also consistent with the catenary cable model described in the Supplemental Material [54], which shows that nonlinear FxE responses are a consequence of linear flexoelectricity in a nonlinear elastic system. Note that this is distinct from nonlinear flexoelectricity.

IV. CONCLUSION

In summary we have found that extrinsic contributions to flexoelectricity originating from strain-gradient-induced TB polarization are substantial and can surpass intrinsic contributions to flexoelectricity in twinned LAO. This experimentally confirms the importance of microstructure in FxE phenomena. The FxE characterization of twin-free LAO crystals suggests an intrinsic effective flexocoupling voltage ~14 V, which is enhanced to ~55 V at elevated temperatures due to TB FxE contributions. These extrinsic contributions are sensitive to the details of TB microstructure and responsible for previously unobserved anelastic and nonlinear FxE responses at room temperature in LAO. These findings directly demonstrate that structural defects, and their deformation mechanisms, are important in macroscopic FxE responses.

[1] S. Trolier-McKinstry, S. Zhang, A. J. Bell, and X. Tan, Annu. Rev. Mater. Res. **48**, 191 (2018).

[2] M. Demartin Maeder, D. Damjanovic, and N. Setter, J. Electroceram. **13**, 385 (2004).

[3] P. V. Yudin and A. K. Tagantsev, Nanotechnology **24**, 432001 (2013).

[4] P. Zubko, G. Catalan, and A. K. Tagantsev, Annu. Rev. Mater. Res. **43**, 387 (2013).

[5] W. Ma and L. E. Cross, Appl. Phys. Lett. **78**, 2920 (2001).

[6] J. Narvaez, F. Vasquez-Sancho, and G. Catalan, Nature (London) **538**, 219 (2016).

[7] L. M. Garten and S. Trolier-McKinstry, J. Appl. Phys. **117**, 094102 (2015).

[8] J. Narvaez and G. Catalan, Appl. Phys. Lett. **104**, 162903 (2014).

[9] X. Zhang, Q. Pan, D. Tian, W. Zhou, P. Chen, H. Zhang, and B. Chu, Phys. Rev. Lett. **121**, 057602 (2018).

[10] R. Resta, Phys. Rev. Lett. **105**, 127601 (2010).

[11] J. W. Hong and D. Vanderbilt, Phys. Rev. B **88**, 174107 (2013).

[12] M. Stengel, Nat. Commun. **4**, 2693 (2013).

[13] M. Stengel, Phys. Rev. B **88**, 174106 (2013).

[14] C. E. Dreyer, M. Stengel, and D. Vanderbilt, Phys. Rev. B **98**, 075153 (2018).

[15] P. Zubko, G. Catalan, P. R. L. Welche, A. Buckley, and J. F. Scott, Phys. Rev. Lett. **99**, 167601 (2007).

[16] G. Lu, S. Li, X. Ding, and E. K. H. Salje, Appl. Phys. Lett. **114**, 202901 (2019).

[17] G. Lu, S. Li, X. Ding, J. Sun, and E. K. H. Salje, Phys. Rev. Mater. **3**, 114405 (2019).

[18] G. Lu, S. Li, X. Ding, J. Sun, and E. K. H. Salje, Sci. Rep. **9**, 15834 (2019).

[19] H. D. Megaw and C. N. W. Darlington, Acta Crystallogr. A **31**, 161 (1975).

[20] S. A. Hayward *et al.*, Phys. Rev. B **72**, 054110 (2005).

[21] S. Bueble, K. Knorr, E. Brecht, and W. W. Schmahl, Surf. Sci. **400**, 345 (1998).

[22] S. Bueble and W. W. Schmahl, Mater. Struct. **6**, 140 (1999).

[23] X. Wang, U. Helmersson, J. Birch, and N. Wei-Xin, J. Cryst. Growth **171**, 401 (1997).

[24] K. Aizu, Phys. Rev. B **2**, 754 (1970).

[25] J. Sapriel, Phys. Rev. B **12**, 5128 (1975).

[26] R. J. Harrison and S. A. T. Redfern, Phys. Earth Planet. Inter. **134**, 253 (2002).

[27] R. J. Harrison, S. A. T. Redfern, A. Buckley, and E. K. H. Salje, J. Appl. Phys. **95**, 1706 (2004).

[28] R. J. Harrison, S. A. T. Redfern, and E. K. H. Salje, Phys. Rev. B **69**, 144101 (2004).

[29] E. K. H. Salje and M. A. Carpenter, Appl. Phys. Lett. **99**, 051907 (2011).

[30] S. Kustov, Iu. Liubimova, and E. K. H. Salje, Appl. Phys. Lett. **112**, 042902 (2018).

[31] S. Puchberger, V. Soprunyuk, W. Schranz, and M. A. Carpenter, Phys. Rev. Mater. **2**, 013603 (2018).

[32] D. G. Schlom, L.-Q. Chen, C.-B. Eom, K. M. Rabe, S. K. Streiffer, and J.-M. Triscone, Annu. Rev. Mater. Res. **37**, 589 (2007).

[33] D. G. Schlom, L.-Q. Chen, C. J. Fennie, V. Gopalan, D. A. Muller, X. Pan, R. Ramesh, and R. Uecker, MRS Bull. **39**, 118 (2014).

[34] G. Catalan *et al.*, Nat. Mater. **10**, 963 (2011).

[35] D. Lee, A. Yoon, S. Y. Jang, J.-G. Yoon, J.-S. Chung, M. Kim, J. F. Scott, and T. W. Noh, Phys. Rev. Lett. **107**, 057602 (2011).

[36] P. Koirala, C. A. Mizzi, and L. D. Marks, Nano Lett. **18**, 3850 (2018).

[37] A. Ohtomo and H. Y. Hwang, Nature (London) **427**, 423 (2004).

[38] P. Sharma *et al.*, Nano Lett. **15**, 3547 (2015).

[39] A. Raslan and W. A. Atkinson, Phys. Rev. B **98**, 195447 (2018).

[40] F. Zhang *et al.*, Phys. Rev. Lett. **122**, 257601 (2019).

[41] Note that twin boundaries in LAO are crystallographically equivalent to domain walls in ferroelastic materials.

[42] E. A. Eliseev, A. N. Morozovska, Y. Gu, A. Y. Borisevich, L.-Q. Chen, V. Gopalan, and S. V. Kalinin, Phys. Rev. B **86**, 085416 (2012).

[43] R. Ahluwalia, A. K. Tagantsev, P. Yudin, N. Setter, N. Ng, and D. J. Srolovitz, Phys. Rev. B **89**, 174105 (2014).

[44] Y. Gu, M. Li, A. N. Morozovska, Y. Wang, E. A. Eliseev, V. Gopalan, and L.-Q. Chen, Phys. Rev. B **89**, 174111 (2014).

[45] E. A. Eliseev, I. S. Vorotiahin, Y. M. Fomichov, M. D. Glinchuk, S. V. Kalinin, Y. A. Geneko, and A. N. Morozovska, Phys. Rev. B **97**, 024102 (2018).

[46] G. Catalan, J. Seidel, R. Ramesh, and J. F. Scott, Rev. Mod. Phys. **84**, 119 (2012).

[47] E. K. H. Salje, S. Li, M. Stengel, P. Gumbsch, and X. Ding, Phys. Rev. B **94**, 024114 (2016).

[48] E. K. H. Salje, M. Alexe, S. Kustov, M. C. Weber, J. Schiemer, G. F. Nataf, and J. Kreisel, Sci. Rep. **6**, 27193 (2016).

[49] H. Yokota, S. Matsumoto, E. K. H. Salje, and Y. Uesu, Phys. Rev. B **98**, 104105 (2018).

[50] S. Van Aert, S. Turner, R. Delville, D. Schryvers, G. Van Tendeloo, and E. K. H. Salje, Adv. Mater. **24**, 523 (2012).

[51] E. K. H. Salje, O. Aktas, M. A. Carpenter, V. V. Laguta, and J. F. Scott, Phys. Rev. Lett. **111**, 247603 (2013).

[52] L. Goncalves-Ferreira, S. A. T. Redfern, E. Artacho, and E. K. H. Salje, Phys. Rev. Lett. **101**, 097602 (2008).

[53] A. Schiaffino and M. Stengel, Phys. Rev. Lett. **119**, 137601 (2017).

[54] See Supplemental Material at http://link.aps.org/supplemental/ 10.1103/PhysRevMaterials.5.064406 for experimental details of flexoelectric characterization, a justification for approximating LaAlO$_3$ as a cubic material, derivations of effective flexoelectric coefficients with and without twins, a discussion of the catenary cable model, optical imaging before and after flexoelectric measurements, additional measurements showing anelasticity, and a discussion of sample-to-sample-variations. This includes additional Refs. [61–68].

[55] The convention adopted for this work is $P_i = \mu_{ijkl}\epsilon_{kl,j}$. Therefore, μ_{zzzz} and μ_{zzxx} correspond to the longitudinal and transverse cubic flexoelectric coefficient tensor components, respectively.

[56] X. Luo and B. Wang, J. Appl. Phys. **104**, 073518 (2008).

[57] J. Chrosch and E. K. H. Salje, J. Appl. Phys. **85**, 722 (1999).

[58] J. Narvaez, S. Saremi, J. Hong, M. Stengel, and G. Catalan, Phys. Rev. Lett. **115**, 037601 (2015).

[59] A. Abdollahi, F. Vasquez-Sancho, and G. Catalan, Phys. Rev. Lett. **121**, 205502 (2018).

[60] M. Mundschau, E. Bauer, and W. Teleips, Surf. Sci. **223**, 413 (1989).

[61] O. A. Bauchau and J. I. Craig, *Structural Analysis* (Springer, Dordrecht, 2009).

[62] W. Schranz, Phase Transitions **64**, 103 (1997).

[63] S. K. Kaldor and I. C. Noyan, Appl. Phys. Lett. **80**, 2284 (2002).

[64] G. F. C. Searle, *Experimental Elasticity*, 2nd ed. (Cambridge University Press, Cambridge, UK, 1920).

[65] P. Delugas, V. Fiorentini, and A. Filippetti, Phys. Rev. B **71**, 134302 (2005).

[66] L. D. Landau and E. M. Lifshitz, *Theory of Elasticity*, 2nd ed. (Pergamon, New York, 1970).

[67] M. Stengel, Phys. Rev. B **90**, 201112(R) (2014).

[68] A. V. Kityk, W. Schranz, P. Sondergeld, D. Havlik, E. K. H. Salje, and J. F. Scott, Phys. Rev. B **61**, 946 (2000).